EDINBURGH INSTRUMENTS

50 YEARS 1971-2021

PRECISION RAMAN

Best-in-class Raman microscopes
for research and analytical requirements backed with world-class customer support and service.

edinst.com

Research Article

Journal of RAMAN SPECTROSCOPY

Received: 8 June 2009 Accepted: 28 August 2009 Published online in Wiley Interscience: 13 November 2009

(www.interscience.wiley.com) DOI 10.1002/jrs.2520

FT-Raman, FT-IR spectral and DFT studies on 6, 8-dichloroflavone and 6, 8-dibromoflavone

Yusuf Erdogdu,[a]* Ozan Unsalan[b] and M. Tahir Gulluoglu[a]

In this study, experimental and theoretical vibrational spectral results of the molecular structures of 6,8-dichloroflavone (6,8-dcf) and 6,8-dibromoflavone (6,8-dbf) are presented. The FT-IR and FT-Raman spectra of the compounds have been recorded together between 4000 and 400 cm^{-1} and 3500–5 cm^{-1} regions, respectively. The molecular geometry and vibrational wavenumbers of 6,8-dcf and 6,8-dbf in their ground state have been calculated by using DFT/B3LYP functional, with 6-31++G(d,p) basis set used in calculations. All calculations were performed with Gaussian03 software. The obtained vibrational wavenumbers and optimized geometric parameters were seen to be in good agreement with the experimental data. Scale factors have been used in order to compare how the calculated and experimental data are in agreement. Theoretical infrared intensities are also reported.

Supporting information may be found in the online version of this article.

Keywords: infrared spectra; Raman spectra; density functional theory; 6,8-dichloroflavone and 6,8-dibromoflavone

Introduction

Flavonoids are a large group of secondary plant metabolites that share a basic phenylbenzopyrone feature and are found in all vascular plants in which they occur in several structurally and biosynthetically related classes.[1] They are important constituents of the human diet[2] and can also be found in expressive amounts in many medicinal plants.[3] Flavonoids are members of a class of widely distributed biological natural products containing aromatic heterocyclic skeleton of flavan but no nitrogen. Generally, flavonoids are biological pigments providing colors ranging from red to blue in flowers, fruit and leaves. Besides their coloring properties in plants, flavonoids have important roles in the growth and development of plants; protection against UV-B radiation; formation of antifungal barriers; antimicrobial, insecticidal and oestrogenic activities; and plant reproduction. Flavonoids also exhibit a wide range of biological properties including anti-microbial, insecticidal and oestrogenic activities.[4]

In the present work we report calculated and experimental (FT-IR and FT-Raman) spectral results of the 6,8-dcf and 6,8-dbf molecules by using DFT/B3LYP approximations. To the best of our knowledge, neither detailed quantum chemical calculations nor the vibrational spectra of 6,8-dcf and 6,8-dbf have been reported. Therefore, the present investigation was undertaken to study the vibrational spectra of these molecules completely and to identify the various modes with greater wavenumber accuracy. Density functional theory (DFT) calculations have been performed to support our wavenumber assignments. Furthermore, we interpreted the calculated spectra in terms of potential energy distributions (PED) and made the assignments of the each vibrational mode according to the PED analysis results.

Experimental

The 6,8-dcf and 6,8-dbf samples were purchased from ABCR Chemical Company with a stated purity of greater than 98% and they were used as such without further purification. The samples are in powder form at room temperature. The infrared spectra of the samples were recorded between 400 cm^{-1} and 4000 cm^{-1} on a Mattson 1000 FT-IR spectrometer which was calibrated using polystyrene bands. The samples were prepared as KBr discs. The FT-Raman spectrum of the samples were recorded between 5 and 3500 cm^{-1} region on a Bruker FRA 106/S FT-Raman instrument using 1064 nm excitation from an Nd : YAG laser. The detector was a liquid nitrogen cooled Ge detector.

Computational Details

The Gaussian 03W and Gauss-view molecular visualization[5,6] software package was used for the theoretical calculations. The quantum chemical calculations were performed applying the DFT (B3LYP) with 6-31++G(d,p) basis set. The geometry optimizations were carried out by wavenumber calculations using same basis sets. The calculated wavenumbers were scaled with scaling factors. The vibrational modes were assigned on the basis of PED analysis using VEDA[7] software.

Result and Discussion

Conformational analysis

While the conjugative interaction between the C ring, and the A and B rings tends to prefer a planar structure, the steric repulsion between the *ortho*-ring hydrogens favors a non-planar structure.

* *Correspondence to: Yusuf Erdogdu, Department of Physics, Ahi Evran University, 40040 Kirsehir, Turkey. E-mail: yusuferdogdu@gmail.com*

a *Department of Physics, Ahi Evran University, 40040 Kirsehir, Turkey*

b *Department of Physics, Istanbul University, 34134 Fatih/Istanbul, Turkey*

Journal of RAMAN SPECTROSCOPY

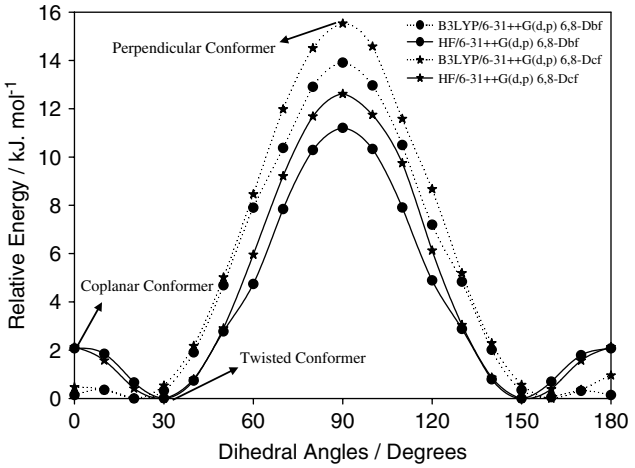

Figure 1. Torsional barriers for 6,8-dichloroflavone and 6,8-dibromoflavone.

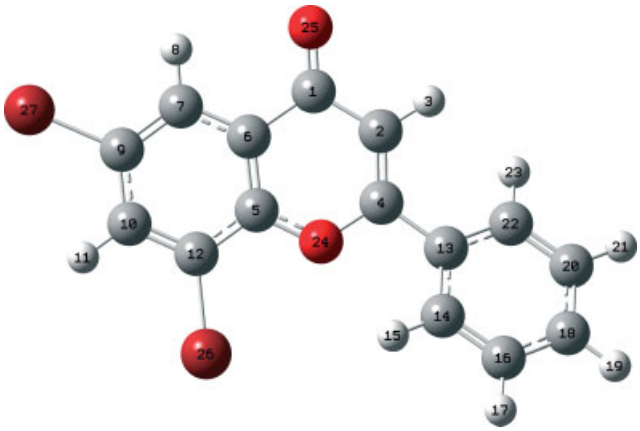

Figure 2. Structure and atom numbering of 6,8-dichloroflavone and 6,8-dibromoflavone.

The equilibrium geometry of the molecules results from a balance between these two effects. Figure 1 shows the variation of torsional barriers *versus* dihedral angles. The calculated relative energies for torsional angle are given in Table S1 (Supporting Information). The torsional barrier for phenyl rotation computed by using the B3LYP and HF with 6-31++G(d,p) basis set corresponds to a low-transition state at 0° (coplanar conformation) and high-transition state at 90° (perpendicular conformation). In both models, the relative energies of corresponding molecules have the same trends with the uniform shapes of torsional dependence.

In the flavonoid derivative, the four minima occurring at the torsional angles are identical because the phenyl group has no substituent at either the *ortho* (*o*) or *meta* (*m*) positions. For this reason, it was satisfactory to optimize only one of the four equivalent minima.[8]

$$(0+\alpha),\ (180-\alpha),\ (180+\alpha),\ (360-\alpha).$$

Molecular orbital energies

The highest occupied molecular orbital (HOMO), the lowest unoccupied molecular orbital (LUMO), and the energy gap between HOMO and LUMO for 6,8-dcf and 6,8-dbf molecules calculated by the B3LYP/6-31++G(d,p) level of theory are shown in Figs S1 and S2 (Supporting Information). All conformations of the 6,8-dcf molecule of identical HOMO energies were computed. Relative to the twisted 6,8-dbf conformer, the HOMO energy decreases by 0.027 eV in the coplanar and perpendicular conformations. The LUMO energies of 6,8-dcf and 6,8-dbf molecules were computed and found to be identical. However, $\Delta E_{HOMO-LUMO}$ energies of 6,8-dcf molecule are larger than those of 6,8-dbf molecule.

In Figs S1 and S2 (Supporting Information), the dependence of the HOMO and LUMO on the molecular conformation is shown. The HOMO of the all conformations of both molecules is distributed over benzopyrone ring (A, B rings and halogen atoms). The LUMO is located over the all rings without halogen atoms for coplanar and twisted conformations, whereas it is distributed over benzopyrone ring without halogen atoms.

Geometry optimization

Optimized molecular structures of the 6,8-dcf and 6,8-dbf were calculated using DFT/B3LYP levels of theory using 6-31++G(d,p) standard basis set. Calculated geometric parameters and definitions of the natural coordinates for the molecules are summarized in Table S2 (Supporting Information). To the best of our knowledge, crystal data of 6,8-dcf and 6,8-dbf are not available in the literature. Therefore, optimized geometric parameters of 6,8-dcf and 6,8-dbf were compared with those of flavone[9] and 3, 30-[*o*-phenylenebis(methyleneoxy)]-bis(6-chlorofavone).[10] By taking into account the fact that the molecular geometry in the vapour phase may be different from that in its solid phase, owing to extended hydrogen bonding and stacking interactions it can be seen that there is reasonable agreement between calculated and experimental geometric parameters. Crystal structure data of flavone[9] were also used for 6,8 dcf and 6,8 dbf due to their skeletal analogy. Because of having neither reflection plane nor inversion center, calculations utilized the C_1 symmetries of the compounds (Fig. 2).

When the $O_{24}-C_4-C_{13}-C_{14}$ dihedral angle increased, it was seen that the C_4-C_{13} bond length increased. The $O_{24}-C_4-C_{13}-C_{14}$ dihedral angles are 3.1° (5,7-dihydroxy-4′-methoxyflavone),[11] 5.2° (5-hydroxyflavone),[12] 8.2° (flavone-3′-sulfonamide),[13] 139.8° (2′-methyl-3′-nitroflavone)[14] and 164.4° (5,4-dihydroxy-3,6,7,8-tetramethoxyflavone)[15] in the x-ray data. The C–C bond lengths of these molecules are 1.453 Å° (5,7-dihydroxy- 4′-methoxyflavone),[11] 1.465 Å (5-hydroxyflavone),[12] 1.478 Å (flavone-3′-sulfonamide),[13] 1.491 Å (2′-methyl-3′-nitroflavone)[14] and 1.503 Å (5,4′-dihydroxy-3,6,7,8-tetramethoxyflavone)[15] in the x-ray data.

The dihedral angle between the phenyl and γ-pyrone ring is small as expected in the generally preferred conformation of flavones. The O_{24}-C_4-C_{13}-C_{14} dihedral angle of flavone is 10.53° on the basis of x-ray data[9] and 19° (161°) as calculated by B3LYP/6-31G(d).[16] The $O_{24}-C_4-C_{13}-C_{14}$ dihedral angles of 6,8-dcf and 6,8-dbf are 17.49° and 18.29°, respectively by B3LYP/6-31++G(d,p).

C_4-C_{13} bond lengths calculated by B3LYP/6-31++G(d,p) level of theory are1.474 Å (6,8-dcf) and 1.473 Å (6,8-dbf). This bond length is 1.475 Å for the flavone skeleton.[9] With the halogen substitution, lengths of this bond for 6,8-dcf and 6,8-dbf molecules were predicted to be slightly shorter (1.473 Å) in B3LYP results than the corresponding bond distance of flavone. This result indicates that this bond length is not affected at all when halogen substitution exists. Also $C_1{=}O_{25}$ (1.226 Å for free flavone) bond length is not affected at all. This bond length is 1.232 Å for 6,8-dcf,

1.224 Å for 6,8-dbf and 1.226 Å for flavone according to the B3LYP results. Predicted C_5-O_{24} bond length for both 6,8-dcf and 6,8-dbf is 1.360 Å by B3LYP and in the corresponding experimental data it is 1.371 Å. $O_{24}-C_4-C_{13}-C_{14}$ dihedral angle of 6,8-dcf and 6,8-dbf molecules is predicted to be slightly smaller than the corresponding dihedral angle of flavone. This value for flavone is 19° by B3LYP/6-31G(d)[16] level of theory, while it is 18.24° (6,8-dcf) and 18.93° (for 6,8-dbf) by the B3LYP/6-31++G(d,p) level of theory. When B3LYP results are considered, maximum deviation of bond lengths from experimental data for both 6,8-dcf and 6,8-dbf is 0.015 Å and deviations from bond angles are 0.22° and 2.2°, respectively. The most significant difference was seen in bond lengths of C–Cl and C–Br. While C_9-Cl_{26} bond length was predicted as 1.754 Å by B3LYP, corresponding C_9-Br_{26} bond length is 1.913 Å. While $C_{12}-Cl_{27}$ bond length is 1.746 Å, $C_{12}-Br_{27}$ bond length is 1.906 Å. These results show how flavone skeleton was affected by Cl or Br substitution.

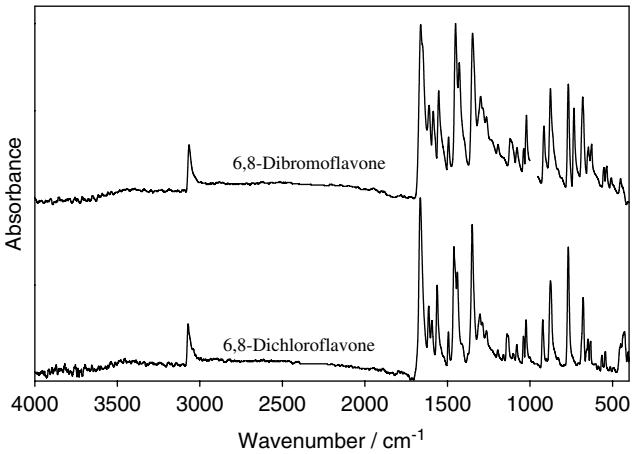

Figure 4. The infrared spectra of the 6,8-dichloroflavone and 6,8-dibromoflavone (in KBr).

Assignment of fundamentals

Both 6,8-dcf and 6,8-dbf molecules consist of 27 atoms, which have 75 normal modes. To the best of our knowledge, there have been no detailed quantum chemical studies carried out for the vibrational spectra of 6,8-dcf and 6,8-dbf. All the calculated values in each method are overestimated, as well known in theoretical assignment for hydrocarbons. Figures 3 and 4 present the FT-Raman and FT-IR spectra of 6,8-dcf and 6,8-dbf, respectively. The experimental FT-IR and FT-Raman wavenumbers are tabulated in Table 1 together with the calculated wavenumbers. As seen in the tables, IR absorption intensities of 6,8-dcf and 6,8-dbf are in consistency with the PED results.[7]

The Raman activities (S_i) calculated with Gaussian 03 program were converted to relative Raman intensities (I_i) using the following relationship derived from the intensity theory of Raman scattering.[17]

$$I_i = \frac{f(\upsilon_0 - \upsilon_i)^4 S_i}{\upsilon_i[1 - \exp(hc\upsilon_i/kt)]}$$

where υ_0 is the exciting wavenumber in cm^{-1}, υ_i the vibrational wavenumber of the ith normal mode, h, c and k are fundamental constants and f is a suitably chosen common normalization factor for all peak intensities.

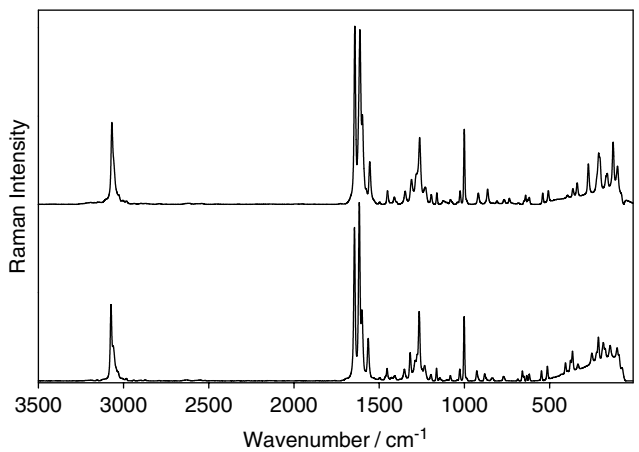

Figure 3. Raman spectra of the 6,8-dichloroflavone (above) and 6,8-Dibromoflavone (below).

Only one CH stretching mode of 6,8-dcf for ring B was calculated at 3100 cm^{-1} by the B3LYP level of theory. This mode was observed experimentally at 3071 cm^{-1} and 3073 cm^{-1} in FT-IR and FT-Raman spectra, respectively. The CH stretching mode for the ring B was calculated at 3155 cm^{-1} and assigned at 3066 cm^{-1} (IR) and 3067 cm^{-1} (Ra) in the 6,8-dbf. For the free flavone these values correspond to 3100 cm^{-1} (IR) and 3135 cm^{-1} (Ra). It can be seen from these results that this shift to lower value of CH stretching mode shows how this mode is affected by halogen substitution.

Two CH stretching modes for ring A of 6,8-dbf were calculated at 3146 cm^{-1} (3090 cm^{-1} for 6,8-dcf) and 3142 cm^{-1} (3086 cm^{-1} for 6,8-dcf) by B3LYP but were not observed in either FT-IR or FT-Raman spectra.

Three of five of the CH stretching modes for ring C of 6,8-dbf were calculated at 3140 cm^{-1} (3083 cm^{-1} for 6,8-dcf), 3127 cm^{-1} (3070 cm^{-1} for 6,8-dcf) and 3119 cm^{-1} (3062 cm^{-1} for 6,8-dcf). The other two CH stretching modes for ring C of 6,8-dbf were calculated at 3109 cm^{-1} (3052 cm^{-1} for 6,8-dcf) and 3099 cm^{-1} (3043 cm^{-1} for 6,8-dcf), and observed in IR at 3028 cm^{-1} (3025 cm^{-1} for 6,8-dcf, 3070 cm^{-1} for free flavone) and in Raman at 3026 cm^{-1} (3030 cm^{-1} for 6,8-dcf, 3070 cm^{-1}-IR for free flavone). The last CH stretching mode for ring C was observed at 2982 cm^{-1} for 6,8-dbf (3040 cm^{-1} for the free flavone) in both IR and Raman spectra and calculated at 3099 cm^{-1}. These shifts to lower values show that these CH stretching modes for ring C are sensitive to halogen substitution.

The characteristic C=O stretching mode was calculated at 1671 cm^{-1} by B3LYP and observed at 1663 cm^{-1} (IR-1665 cm^{-1} for 6,8-dcf), 1642 cm^{-1} (Ra-1644 cm^{-1} for 6,8-dcf) for 6,8-dbf, where as the corresponding values for the free flavones were 1646 cm^{-1} and 1633 cm^{-1} in FT-IR and FT-Raman spectra, respectively. The C=O stretching vibrations shifted to higher wavenumber region by halogen substitution. This means that C=O stretching vibration is also very sensitive to halogen coordination.

In the FT-IR spectrum two of three C–C stretching vibrations for ring B were observed at 1613 cm^{-1} (1613 cm^{-1}-Ra, B3LYP-1610 cm^{-1}). The other ring stretching mode for ring B was only observed at 1408 cm^{-1} (B3LYP-1394 cm^{-1}) in the FT-Raman spectrum. Corresponding values for 6,8-dcf were 1616 cm^{-1}-IR (1617 cm^{-1}-Ra) and 1414 cm^{-1}-IR (1424 cm^{-1}-Ra).

Table 1. Comparison of the observed and calculated vibrational spectra of free 6,8-dichloroflavone and 6,8-dibromoflavone

	6,8-Dichloroflavone							6,8-Dibromoflavone						
	B3LYP/6-31++G(d.p)							B3LYP/6-31++G(d.p)						
	Wavenumber[a]	Wavenumber[b]	I_{IR}[c]	I_{RA}[d]	EXP IR	EXP RA	TED[e]	Wavenumber[a]	Wavenumber[b]	I_{IR}[c]	I_{RA}[d]	EXP IR	EXP RA	TED[e]
ν_1	27	26	0.002	3.500			$\tau_{(AB-C)}$(94)	25	24	0.105	2.751			τ_{ring} (BC) (40) + τ_{CCCO} (21)
ν_2	33	32	0.119	0.173			$\gamma_{(AB-C)}$(67)	30	30	0.054	2.897			τ_{ring} (AB–C) (73)
ν_3	79	77	0.026	0.363			$\delta_{(AB-C)}$(64)	67	65	0.034	0.408		101 w	τ_{ring} (AB–C) (66)
ν_4	93	91	0.221	0.090		103 w	$\tau_{(AB)}$ + $\gamma_{(BC)}$(52)	86	84	0.183	0.196			τ_{BC} (30) + $\tau_{CCC=O}$ (18) + τ_{CCCBr} (6)
ν_5	121	118	0.013	0.169			$\tau_{(AB)}$ (30) + τ_{Cl-CCC} (28)+$\tau_{(BC)}$(11)	106	103	0.003	0.178			δ_{CC-Br} (83)
ν_6	163	160	0.847	0.160		143 w	τ_{Cl-CCC}(17) + $\tau_{CCC=O}$(15) + τ_{COCC}(14)	119	117	0.010	0.275		126 m	τ_{CCC-Br} (44) + τ_{AB} (15) + τ_{COCC} (9)
ν_7	179	175	0.027	0.245			δ_{Cl-CC}(77)	152	148	0.198	25.12			δ_{CCO} (AB) (14) + δ_{BrCC} (13) + δ_{CCC} (BC) (12)
ν_8	183	179	0.190	0.164			δ_{Cl-CC}(25) + δ_{CC-O}(AB) (11)	154	151	0.568	49.74		161 w	τ_{ring} (B) (23) + $\tau_{CCC=O}$ (17) + τ_{BrCCC} (14)
ν_9	201	196	0.108	0.180			τ_{ring}(AB) (69)	188	184	0.176	24.43			ν_{C-Br} (17) + ν_{CC} (BC) (8) + τ_{ring} (BC) (6)
ν_{10}	222	217	0.069	0.224		213 m	τ_{ring}(C) (21) + τ_{ring}(BC) (13)	206	201	0.089	55.47		211 m	τ_{Br-CCC} (24) + τ_{ring} (AB) (22)
ν_{11}	250	244	0.218	0.295		251 w	ν_{CC}(BC) (17) + ν_{C-O}(7) + δ_{CCC}(BC) (7)	224	220	0.244	27.79			τ_{CCCC} (BC) (12) + δ_{CCC} (BC) (11)
ν_{12}	327	320	0.472	9.342		332 w	$\delta_{CC=O}$(24) + ν_{C-Cl}(14) + ν_{ring}(B) (12)	264	258	0.134	31.67		271 m	ν_{C-Br} (38) + $\delta_{CC=O}$ (12) + δ_{ring} (A) (7)
ν_{13}	361	353	0.083	22.36			τ_{CCC}(10) + ν_{C-Cl}(8) + δ_{CC-Cl}(7)	335	328	0.005	13.50		336 w	δ_{CCC} (BC) (20) + ν_{C-Br} (11) + ν_{CC} (BC) (10)
ν_{14}	377	368	0.181	9.281			τ_{CCC-O}(12) + δ_{CCC}(BC) (7) + τ_{CCC-Cl}(6)	356	349	0.535	5.543			$\delta_{CC=O}$ (19) + δ_{CCBr} (11) + δ_{CCC} (AB) (9)
ν_{15}	405	395	1.926	9.767			ν_{C-Cl}(32) + δ_{ring}(A) (13) + δ_{CC-Cl}(10)	364	356	1.524	5.374		363 vw	τ_{ring} (AB) (80)
ν_{16}	411	402	0.055	4.420	405 w	406 w	τ_{ring}(C) (95)	395	386	0.864	0.683		394 vw	δ_{CCBr} (18) + ν_{C-Br} (15) + δ_{ring} (A) (7)
ν_{17}	433	423	0.781	1.738	428 s		ν_{C-C}(18) + δ_{CCCl}(16) + δ_{ring}(A) (16)	410	401	0.062	3.647			τ_{CCCC} (C) (61) + τ_{CCCH} (30)
ν_{18}	474	463	1.191	0.350	451 vw		τ_{CCCH}(C) (17) + τ_{ring}(C) (16)	467	456	0.820	0.378	452 w		$\tau_{CCC=O}$ (20) + τ_{CCCBr} (15)
ν_{19}	487	476	0.296	0.958	493 w		τ_{ring}(A) (26) + τ_{CCCH}(A) (9)	480	469	0.367	0.977			τ_{CCCH} (40) + τ_{CCCC} (C) (20)
ν_{20}	517	505	0.368	21.48	513 w	512 m	δ_{CCC}(B) (28) + δ_{COC}(16) + $\delta_{CC=O}$(10)	514	502	0.437	19.31	507 w	506 w	δ_{ring} (B) (72)
ν_{21}	553	541	1.644	6.968	543 m	546 w	$\delta_{CC=O}$(15) + δ_{ring}(B)(13) + δ_{CC-Cl}(11)	546	534	1.674	8.557	535 w	540 w	δ_{ring} (A) (16) + δ_{ring} (B) (13) + δ_{CCBr} (12)

Journal of RAMAN SPECTROSCOPY

Table 1. (*Continued*)

	6,8-Dichloroflavone							6,8-Dibromoflavone						
	B3LYP/6-31++G(d.p)							B3LYP/6-31++G(d.p)						
	Wavenumber[a]	Wavenumber[b]	I_{IR}[c]	I_{RA}[d]	EXP IR	EXP RA	TED[e]	Wavenumber[a]	Wavenumber[b]	I_{IR}[c]	I_{RA}[d]	EXP IR	EXP RA	TED[e]
ν_{22}	576	563	0.888	0.076	565 vw		τ_{CCCH}(A) (24)	561	549	0.874	0.224	552 w		δ_{CCC} (C) (56) + δ_{ring} (C) (20)
ν_{23}	631	616	0.104	5.929		618 w	δ_{ring}(C) (55) + δ_{CCH}(C) (25)	632	618	0.574	6.188		618 vw	$\delta_{CC=O}$ (28) + δ_{CC-O} (10) + δ_{CCC} (C) (10)
ν_{24}	639	624	3.095	1.906	633 m	633 w	$\delta_{CC=O}$(29) + δ_{ring}(C) (15)+ δ_{CCO}(AC) (12)	636	622	2.792	2.278	627 w	627 vw	τ_{CCCC} (C) (13) + ν_{Br-C} (9)
ν_{25}	662	647	0.944	5.526			δ_{ring}(C) (21)	649	635	2.116	10.32	647 w	639 vw	τ_{ring} (C) (20) + τ_{COCC} (9) + τ_{OCCC} (8)
ν_{26}	669	653	1.498	5.380			ν_{C-Cl}(5) + τ_{CC-O-C}(5) + τ_{CCCH}(BC) (4)	666	651	1.620	2.086			τ_{ring} (A) (64)
ν_{27}	685	669	0.101	0.859	677 s	685 vw	τ_{ring}(A) (14) + τ_{CCCC}(AB) (10)	683	668	0.128	1.175			τ_{ring} (C) (59)
ν_{28}	701	685	8.489	0.224			τ_{CCCH}(C) (53) + τ_{ring}(C) (30)	702	687	8.645	0.164	681 s		ν_{C-Br} (25) + ν_{CC} (BC) (8) + δ_{CCC} (A) (8)
ν_{29}	761	744	0.127	0.455			τ_{ring}(B) (15) + τ_{ring}(A) (12) + $\tau_{CCC=O}$(12)	739	723	14.17	3.486			τ_{ring} (B) (49)
ν_{30}	774	756	16.927	1.906			ν_{C-Cl}(26) + ν_{CC}(BC) (7) + ν_{C-O}(6)	764	748	0.127	0.726	733 s	735 w	τ_{CCCH} (45) + τ_{CCCC} (7)
ν_{31}	787	769	8.141	1.759	768 vs	770 vw	γ_{CH}(C) (67)	788	770	8.114	1.972	768 s	766 vw	ν_{ring} (B) (36) + ν_{Br-C} (15) + δ_{ring} (A) (12)
ν_{32}	841	822	1.805	2.453	828 vw	834 w	ν_{C-Cl}(24) + ν_{ring}(B) (19) + δ_{CCC}(A) (10)	814	796	0.381	1.975		809 vw	τ_{CCCC} (A) (34) + τ_{BrCCO} (13) + τ_{CCCH} (A) (12)
ν_{33}	856	836	0.737	0.611			γ_{CH}(C) (73) + τ_{CCCH}(BC) (16)	854	835	0.747	0.695			δ_{ring} (A) (27) + ν_{CC} (B) (8) + ν_{CC} (A) (7)
ν_{34}	873	853	5.175	0.868			τ_{HCCO}(AB) (34) + τ_{CCCH}(BC) (21)	871	852	4.426	6.568			τ_{ring} (C) (56) + τ_{CCCH} (BC) (13)
ν_{35}	886	866	4.342	0.050			γ_{CH}(A) (86)	875	855	3.310	7.408			$\tau_{O=CCH}$ (25) + τ_{CCCH} (BC) (19) + τ_{O-CCH} (11)
ν_{36}	888	868	4.650	7.904	875 s	880 w	δ_{ring}(A) (22) + ν_{C-Cl}(11) + ν_{CC}(B) (10)	888	868	3.755	0.047	877 s	863 m	δ_{COC} (14) + ν_{ring} (C)(10) + δ_{CCO}(9)+δ_{ring}(B)(8)
ν_{37}	929	908	1.026	0.048	899 vw		γ_{CH}(A) (86)	928	907	5.823	5.109			τ_{ring} (C) (88)
ν_{38}	931	910	6.211	4.749			δ_{COC}(13) + ν_{ring}(C) (9) + δ_{ring}(B) (8)	934	913	0.664	0.038	916 s	917 m	ν_{ring} (C) (41) + δ_{ring} (C) (38)
ν_{39}	944	923	0.319	0.248	923 s	926 m	γ_{CH}(C) (68) + τ_{CCCH}(BC) (9)	945	924	0.316	0.156			τ_{ring} (A) (60) + τ_{HCCBr} (33)
ν_{40}	991	968	0.093	0.085			γ_{CH}(C) (75)+τ_{CCCH} (BC) (5)	993	971	0.131	0.138			τ_{HCCH} (C) (50) + τ_{HCCC} (C) (15) + τ_{CCCH} (C) (5)
ν_{41}	1010	987	0.014	0.852	981 vw		γ_{CH}(C) (77)	1010	988	0.033	0.400			ν_{ring} (C) (43) + δ_{CH} (C) (22) + δ_{CCC} (C) (16)

Table 1. (*Continued*)

	6,8-Dichloroflavone							6,8-Dibromoflavone						
	B3LYP/6-31++G(d.p)							B3LYP/6-31++G(d.p)						
	Wavenumber[a]	Wavenumber[b]	I_{IR}[c]	I_{RA}[d]	EXP IR	EXP RA	TED[e]	Wavenumber[a]	Wavenumber[b]	I_{IR}[c]	I_{RA}[d]	EXP IR	EXP RA	TED[e]
ν_{42}	1014	990	0.483	26.67	1001 w	1001 s	δ_{CCH}(C) (41) + ν_{ring}(C) (37)	1016	993	0.335	33.86		1000 s	τ_{ring} (A) (87)
ν_{43}	1045	1021	5.773	9.419	1024 s	1027 m	ν_{ring} (C) (32) + ν_{C-O}(23)	1040	1017	7.226	7.626	1022 s	1025 w	τ_{ring} (C) (77)
ν_{44}	1062	1038	1.841	1.623	1040 w		ν_{ring} (C) (39) + δ_{CCH}(C) (17) + ν_{C-O}(12)	1058	1034	1.444	2.394	1038 w		υ_{CC} (A) (29) + υ_{CO} (21) + δ_{CCH} (C) (8)
ν_{45}	1106	1080	2.757	3.914	1080 w	1081 w	δ_{CCH}(C) (39) + ν_{ring}(C) (26)	1103	1079	2.859	6.695	1079 w	1081 vw	υ_{CC} (C) (50) + δ_{CCH} (C) (32)
ν_{46}	1113	1087	3.104	0.134			ν_{ring}(C) (44) + δ_{CCH}(C) (38)	1110	1086	3.457	0.134			δ_{CCH} (A) (40) + υ_{CC} (C) (32)
ν_{47}	1148	1122	9.784	3.863	1139 m	1144 vw	ν_{CC}(A) (14) + ν_{CC}(B) (14) + ν_{C-Cl}(13)	1127	1102	6.988	4.394			υ_{CC} (A) (67) + δ_{CCH} (A) (7)
ν_{48}	1189	1161	0.166	1.945	1161 w	1162 w	δ_{CCH}(C) (74) + ν_{ring}(C) (15)	1187	1160	0.150	2.078		1160 w	υ_{CC} (C) (54) + δ_{CCH} (C) (15)
ν_{49}	1213	1185	1.007	7.852			δ_{CCH}(C) (67) + ν_{ring}(C) (15)	1210	1183	0.918	10.31			υ_{CC} (C) (65) + δ_{CCH} (A) (7)
ν_{50}	1221	1192	2.208	0.124	1195 w	1194 w	δ_{CCH}(A) (50) + ν_{ring}(A) (14)	1220	1193	3.753	0.091	1195 w	1192 w	δ_{CCH} (C) (73) + υ_{CC} (C) (19)
ν_{51}	1260	1231	0.686	27.71			ν_{ring}(A) (26) + ν_{C-O} (24)+ν_{ring}(B) (17)	1242	1214	0.308	14.61		1227 w	υ_{CC} (A) (42) + δ_{CCH} (A) (24)
ν_{52}	1274	1245	7.956	51.67		1233 w	δ_{CCH}(B) (41) + ν_{CC}(BC)(20) + ν_{ring}(C) (8)	1268	1241	8.584	70.34			δ_{CCH} (C) (51) + υ_{CC} (C) (14) + + υ_{Ring} (13)
ν_{53}	1285	1256	5.303	1.553	1264 w	1264 s	δ_{CCH}(AB) (21) + ν_{ring}(B) (13) + ν_{C-O}(13)	1280	1252	6.040	1.932	1264 vw	1262 s	δ_{CCH} (AB) (40) + υ_{Ring} (24)
ν_{54}	1335	1305	25.59	3.785	1288 vw	1287 vw	ν_{ring}(C) (46) + ν_{C-O}(9)	1324	1295	30.78	4.621	1288 vw		υ_{CC} (AB) (51) + υ_{CO} (26) + δ_{CCH} (A) (21)
ν_{55}	1356	1325	1.656	11.01	1303 vw	1316 m	ν_{ring}(AB) (84)	1336	1306	1.281	15.65	1300 m	1308 m	δ_{CCH} (AB) (47) + υ_{CC} (AB) (14) + υ_{CO} (11) +
ν_{56}	1367	1336	0.511	2.765			δ_{CCH}(C) (47) + ν_{ring}(C) (33)	1357	1327	13.55	1.279			δ_{CCH} (C) (69)
ν_{57}	1377	1345	62.30	14.78	1350 vs	1351 w	δ_{CCH}(C) (24) + ν_{C-O}(14) + δ_{CCH}(B) (8)	1367	1337	49.79	15.96	1348 vs	1347 w	δ_{CCH} (BC) (23) + υ_{CO} (20) + υ_{CC} (AB) (14)
ν_{58}	1439	1406	3.866	3.321	1414 vw	1424 vw	ν_{ring}(A) (33)+ν_{ring}(B) (16) + δ_{CCC}(A) (11)	1425	1394	5.443	4.001		1408 w	υ_{CC} (B) (42) + υ_{CC} (A) (19) + δ_{CCH} (A) (14)

Table 1. (*Continued*)

	6,8-Dichloroflavone							6,8-Dibromoflavone						
	B3LYP/6-31++G(d.p)							B3LYP/6-31++G(d.p)						
	Wavenumber[a]	Wavenumber[b]	I_{IR}[c]	I_{RA}[d]	EXP IR	EXP RA	TED[e]	Wavenumber[a]	Wavenumber[b]	I_{IR}[c]	I_{RA}[d]	EXP IR	EXP RA	TED[e]
ν_{59}	1480	1446	45.01	1.536			ν_{ring}(A) (31) + δ_{CCH}(A) (21) + ν_{C-O} (11)	1464	1432	55.40	1.626	1429 vw		δ_{CCH} (C) (55) + υ_{CC} (C) (20)
ν_{60}	1484	1450	21.48	3.994	1460 vs	1453 w	δ_{CCH}(C) (70) + ν_{ring}(C) (29)	1479	1446	9.133	3.986	1451 vs	1451 w	υ_{CC} (A) (30) + δ_{CCH} (AB) (29) + υ_{CO} (14)
ν_{61}	1531	1496	3.555	2.420	1495 m	1497 vw	δ_{CCH}(C) (62) + ν_{ring}(C) (25)	1525	1492	3.726	2.719	1494 m	1495 vw	δ_{CCH} (C) (61) + ν_{CC} (C) (25)
ν_{62}	1599	1562	24.52	14.42			ν_{ring}(A) (43) + ν_{ring}(B) (29)	1581	1546	21.82	12.47	1553 s	1555 m	υ_{CC} (B) (33) + υ_{CC} (A) (23)
ν_{63}	1621	1584	1.543	8.560	1563 s	1563 m	ν_{ring}(C) (53) + δ_{CCH}(C) (9) + ν_{CC}(B) (7)	1612	1576	1.748	12.53		1574 w	υ_{CC} (C) (54) + ν_{CC}(B) (5)
ν_{64}	1633	1596	6.099	2.258			ν_{ring}(A) (65)	1618	1582	7.652	0.540			υ_{CC} (A) (48) + υ_{CC} (B) (21)
ν_{65}	1650	1612	0.246	35.60	1594 m	1601 vw	ν_{ring}(C) (63) + δ_{CCH} (C) (16)	1642	1606	1.058	55.60	1587 m	1597 w	υ_{ring} (C) (54) + δ_{HCC} (C) (15)
ν_{66}	1654	1616	20.72	100	1614 s	1617 vs	ν_{CC}(B) (50) + ν_{CC}(BC) (6)	1646	1610	22.68	100	1613 m	1613 vs	υ_{CC}(B) (48) + υ_{CC}(BC) (8)
ν_{67}	1717	1677	100	26.46	1665 vs	1644 vs	$\upsilon_{C=O}$(80)	1709	1671	100	25.97	1663 vs	1642 vs	$\upsilon_{C=O}$ (88)
ν_{68}	3187	3043	0.044	0.502	2996 vw	2982 vw	υ_{CH}(C) (99)	3169	3099	0.036	0.525	2982 w	2982 vw	υ_{CH} (C) (99)
ν_{69}	3196	3052	1.426	1.415	3025 vw	3030 vw	υ_{CH}(C) (97)	3179	3109	1.309	1.512	3028 w	3026 vw	υ_{CH} (C) (97)
ν_{70}	3206	3062	3.861	1.650	3039 vw		υ_{CH}(C) (97)	3189	3119	3.344	1.761			υ_{CH} (C) (97)
ν_{71}	3215	3070	2.083	1.603			υ_{CH}(C) (94)	3198	3127	1.793	1.776			υ_{CH} (C) (96)
ν_{72}	3228	3083	0.585	0.826			υ_{CH}(C) (98)	3210	3140	0.612	0.993			υ_{CH} (C) (99)
ν_{73}	3232	3086	1.373	0.529			υ_{CH}(A) (99)	3213	3142	1.534	0.479			υ_{CH} (A) (99)
ν_{74}	3235	3090	0.272	0.833			υ_{CH}(A) (99)	3217	3146	0.442	0.638			υ_{CH} (A) (99)
ν_{75}	3246	3100	0.192	0.877	3071 vs	3073 vs	υ_{CH}(B) (97)	3226	3155	0.178	1.063	3066 vs	3067 vs	υ_{CH} (B) (98)

P, phenyl (C Ring); R, A and B rings; υ, stretching; δ, bending; τ, torsion; vw, very weak; s, strong; m, medium; w, weak; v, very strong.
[a] Unscaled wavenumbers.
[b] Obtained from the wavenumbers calculated at B3LYP/6-31++G(d, p) using scaling factors 0.967 (for wavenumbers under 1800 cm^{-1}) and 0.955 (for those over 1800 cm^{-1}).
[c] Relative absorption intensities normalized with highest peak absorption equal to 100.
[d] Relative Raman intensities calculated by Eqn (1) and normalized to 100.
[e] Total energy distribution calculated B3LYP/6-31++G(d,p) level of theory.

Two of the ring stretching vibrations for ring C were assigned in the FT-IR spectrum at 1587 cm^{-1} (1606 cm^{-1}-B3LYP, 1597 cm^{-1}-Ra) and 916 cm^{-1} (913 cm^{-1}-B3LYP, 917 cm^{-1}-Ra) and only one other was calculated at 988 cm^{-1} by B3LYP. The CC stretching vibrations for ring C were assigned in the FT-Raman spectrum at 1574 cm^{-1} (1576 cm^{-1}-B3LYP), 1160 cm^{-1} (1160 cm^{-1}-B3LYP) and 1081 cm^{-1} (1079 cm^{-1}-B3LYP, 1079 cm^{-1}-IR). One of the CC stretching modes for this ring was calculated at 1183 cm^{-1} by B3LYP. Corresponding values for 6,8-dcf were 1563 cm^{-1} (IR-Ra both), 1185 cm^{-1} by B3LYP, 1161 cm^{-1} (1162 cm^{-1}-Ra) and 1080 cm^{-1}(1081 cm^{-1}-Ra). When bromine was substituted with chlorine it was seen that these vibrational wavenumbers for ring C weren't shifted. This result shows that bromine substitution by chlorine did not affect these vibrations for ring C at all.

Two C–Cl stretching modes were calculated at 822 cm^{-1} (IR-828 cm^{-1}, Ra-834 cm^{-1}) and 653 cm^{-1}. One of the C–Br stretching modes was assigned at 271 cm^{-1} (258 cm^{-1}-B3LYP) in the Raman spectra and another calculated at 184 cm^{-1} by B3LYP. C–Br stretching mode was observed at 681 cm^{-1} in FT-IR spectrum and calculated at 687 cm^{-1} for B3LYP.

The CCH bending modes for ring C were observed at IR-1495 cm^{-1} (IR-1494 cm^{-1} for 6,8-dcf), IR-1460 cm^{-1} (IR-1451 cm^{-1} for 6,8-dcf), IR-1350 cm^{-1} (IR-cm^{-1} for 6,8-dcf), IR-1162 cm^{-1} (Ra-1160 cm^{-1} for 6,8-dcf), IR-1080 cm^{-1} (IR-1079 cm^{-1} for 6,8-dcf) and IR-1001 cm^{-1} (IR-1000 cm^{-1} for 6,8-dcf) for 6,8-dbf. When these values are compared it is seen that there is no significant change in wavenumbers. This means that this vibrational mode is not affected by bromine substitution.

In-plane CCH angle bending modes for both ring A and B were observed experimentally in the FT-IR spectrum at 1300 cm^{-1} (1308 cm^{-1}-Ra, 1306 cm^{-1}-B3LYP) and 1264 cm^{-1} (1262 cm^{-1}-Ra, 1252 cm^{-1}-B3LYP) for 6,8-dbf. When the corresponding values are examined for 6,8-dcf (1303 cm^{-1} and 1264 cm^{-1} in the FT-IR spectrum), it is seen that bromine substitution does not lead to any changes in vibrational wavenumbers of this mode.

The C═O in-plane bending modes were calculated at 320 cm^{-1} (Ra-332 cm^{-1}), 541 cm^{-1} (543 cm^{-1}-IR, 546 cm^{-1}-Ra) and 624 cm^{-1} (633 cm^{-1}-IR, 633 cm^{-1}-Ra) for 68dcf. The only mode observed in the FT-Raman spectrum was at 618 cm^{-1} (618 cm^{-1}-B3LYP). Only one mode was calculated at 349 cm^{-1} for 6,8-dbf. C═O out-of-plane bending mode was observed at IR-452 cm^{-1} (456 cm^{-1}-B3LYP) for 6,8-dbf.

The COC bending mode was calculated at 910 cm^{-1} for 6,8-dcf and was not observed in either FT-IR or FT-Raman spectra. This mode was observed at 877 cm^{-1} and 863 cm^{-1} in the IR and Raman spectra, respectively. This mode was calculated by B3LYP at 868 cm^{-1} for 6,8-dbf. The CCC bending mode of ring B was observed at 513 cm^{-1} and 512 cm^{-1} for FT-IR and FT-Raman spectra, respectively. This mode also was calculated at 505 cm^{-1} by B3LYP level of theory for 6,8-dcf. The in-plane CCC bending between rings B and C was observed in FT-Raman spectrum at 336 cm^{-1} (328 cm^{-1}-B3LYP) and IR-552 cm^{-1} (B3LYP-549 cm^{-1}) for 6,8-dbf.

The out-of-plane CH bending modes for ring C were calculated at 987 cm^{-1} (IR-981 cm^{-1}), 968 cm^{-1} and 923 cm^{-1} (IR-923 cm^{-1}, Ra-926 cm^{-1}), 836 cm^{-1}, 769 cm^{-1} (IR-768 cm^{-1}, Ra-770 cm^{-1}). Two CH out-of-plane bending modes of ring A were calculated at 908 cm^{-1} (899 cm^{-1}-IR) and 866 cm^{-1} for 68dcf. The out-of-plane CH bending mode for ring C was calculated at 971 cm^{-1} by B3LYP for 68dbf. The only one out-of-plane CH bending mode for ring B was calculated at 855 cm^{-1} by B3LYP for 68dbf.

The Br bending modes were assigned at 211 cm^{-1} (ν_{10}), (201 cm^{-1}-B3LYP) and 126 cm^{-1} (ν_6) (117 cm^{-1}-B3LYP) in FT-Raman spectrum. The Cl bending mode was observed at 143 cm^{-1} (ν_6) in the FT-Raman spectrum. The other mode (ν_{10}) was not observed in the FT-Raman spectrum.

Conclusion

The FT-IR and FT-Raman spectra of the title compounds were computed by the B3LYP methods in conjunction with the 6-31++G(d,p) basis set. Results are in good agreement with their observed FT-IR and FT-Raman spectra. Scale factors were used in order to compare how the calculated wavenumbers were consistent with those of the experimental ones. By taking into account small variations of the scaling factors for the derivatives of the title compounds, one can recommend the same scaling factors of the methods mentioned above for future IR and Raman spectral predictions of unknown compounds of this class.

Acknowledgements

This work was supported by the Research Fund of The University of Gazi Project Numbers: 30/2005-01. We wish to thank the central laboratory of METU for Raman spectral recording and Gazi University Art and Science Faculty Department of Chemistry for infrared spectral recording. We wish to thank Assoc. Prof. Dr Mustafa Kurt for the Gaussian 03W program package.

Supporting information

Supporting information may be found in the online version of this article.

References

[1] J. B. Harborne, C. A. Williams, *Phytochemistry* **2000**, *55*(6), 481.
[2] S. Karakaya, N. E. L. Sedef, *Food Chem.* **1999**, *66*(3), 289.
[3] E. Middleton, C. Kandaswami, T. C. Theoharides, Jr *Pharmacol. Rev.* **2000**, *52*(4), 673.
[4] http://chemicalland21.com/fc/FLAVONES.htm.
[5] M. J. Frisch, G. W. Trucks, H. B. Schlegel, G. E. Scuseria, M. A. Robb, J. R. Cheeseman, J. A. Montgomery Jr., T. Vreven, K. N. Kudin, J. C. Burant, J. M. Millam, S. S. Iyengar, J. Tomasi, V. Barone, B. Mennucci, M. Cossi, G. Scalmani, N. Rega, G. A. Petersson, H. Nakatsuji, M. Hada, M. Ehara, K. Toyota, R. Fukuda, J. Hasegawa, M. Ishida, T. Nakajima, Y. Honda, O. Kitao, H. Nakai, M. Klene, X. Li, J. E. Knox, H. P. Hratchian, J. B. Cross, C. Adamo, J. Jaramillo, R. Gomperts, R. E. Stratmann, O. Yazyev, A. J. Austin, R. Cammi, C. Pomelli, J. W. Ochterski, P. Y. Ayala, K. Morokuma, G. A. Voth, P. Salvador, J. J. Dannenberg, V. G. Zakrzewski, S. Dapprich, A. D. Daniels, M. C. Strain, O. Farkas, D. K. Malick, A. D. Rabuck, K. Raghavachari, J. B. Foresman, J. V. Ortiz, Q. Cui, A. G. Baboul, S. Clifford, J. Cioslowski, B. B. Stefanov, G. Liu, A. Liashenko, P. Piskorz, I. Komaromi, R. L. Martin, D. J. Fox, T. Keith, M. A. Al-Laham, C. Y. Peng, A. Nanayakkara, M. Challacombe, P. M. W. Gill, B. Johnson, W. Chen, M. W. Wong, C. Gonzalez, and J. A. Pople, *Gaussian 03, Revision C.02*, Gaussian, Inc.: Wallingford, CT, **2004**.
[6] A. Firsch-, A. B. Nielsen, A. L. Holder, *Gaussview Users Manual*, Gaussian Inc.: Pitsburg, **2000**.
[7] M. H. Jamróz, Vibrational Energy Distribution Analysis VEDA 4, Warsaw, **2004**.
[8] O. Unsalan, Y. Erdogdu, M. Tahir Gulluoglu, *J. Raman Spectrosc.* **2009**, *40*(5), 562.

[9] M. P. Waller, D. E. Hibbs, J. Overgaard, J. R. Hanrahan, T. W. Hambley, *Acta Crystallogr. Sect. A* **2003**, *59*, 767.
[10] S. Thinagar, D. Velmurugan, S. S. Sundara Raj, H.-K. Fun, S. C. Gupta, H. Merazig, S. Bouacida, *Acta Crystallogr. Sect. C* **2003**, *59*, 181.
[11] M. Shoja, *Acta Crystallogr. Sect. C* **1992**, *48*, 2033.
[12] M. Shoja, *Acta Crystallogr. Sect. C* **1990**, *46*, 517.
[13] E. Kendi, S. Özbey, O. Bozdag, R. Ertan, *Acta Crystallogr. Sect. C* **2000**, *56*, 457.
[14] E. Kendi, S. Özbey, M. Tunçbilek, R. Ertan, *Cryst. Res. Technol.* **1996**, *5*, 457.
[15] J. Vijayalakshmi, S. S. Rajan, R. Srinivasan, A. G. Ramachandran Nair, *Acta Crystallogr. Sect. C* **1986**, *42*, 1752.
[16] M. Meyer, *Int. J. Quantum Chem.* **2000**, *76*(6), 724.
[17] R. Wysokinski, K. Hernik, R. Szostak, D. Michalska, *Chem. Phys.* **2007**, *333*, 37.